Tunable Comb-Channels with Orthogonal Polarizations Based on Coupled Resonators and Electro-Optic Effect

Changyun Chen

School of Biochemical & Environmental Engineering, Nanjing Xiaozhuang University, Nanjing, 211171, China

Reprint requests to C. C.; E-mail: cychen@njxzc.edu.cn

Z. Naturforsch. **67a,** 397 – 402 (2012) / DOI: 10.5560/ZNA.2012-0003
Received August 15, 2011 / revised November 18, 2011

We designed a coupled resonator structure and studied its transmission properties through the tight-binding approach and the transfer matrix method. Based on the coupling of resonant modes and the electro-optic effect, some comb-channels with two orthogonal polarizations can be obtained. The total number of channels is two times the number of resonators. The orthogonal polarization channels cannot only be arranged alternately, but also be separated totally, just through adjusting the intensity of the external electric field. The split wavelength interval of two orthogonal polarizations is linear with the intensity of the external electric field.

Key words: Orthogonal Polarizations; Coupled Resonators; Comb-Channels; Electro-Optic Effect.

1. Introduction

In dense wavelength-division multiplexing (DWDM) optical communication, a multi-channeled filter is much needed. Recently, some designs of multi-channeled filters based on the defect mode of photonic crystals (PCs) have been proposed [1 – 6]. By increasing the size or the number of the defects, more and more defect modes with different frequencies will emerge inside the photonic band gap (PBG) as a result of the Bragg resonant, leading to the multi-channeled filtering phenomenon. However, this conventional method has a prominent shortcoming. In order to increase the number of channels and the Q value of the channel, we must increase the number of periods that is at the cost of increasing the volume of the device. In addition, all conventional multi-channeled filters can output only light with one polarization. In practical applications, a multi-channeled filter with two orthogonal polarizations and small volume may be more useful in future optical devices. In this paper, we designed a coupled resonator structure. Based on the coupling of resonant modes and the electro-optic effect, some tunable comb-channels with two orthogonal polarizations can be obtained.

2. Structure Model and Theoretical Methods

The designed structure model is shown in Figure 1. A layered structure of $[\mathrm{DM}]^N\mathrm{D}$ is placed along the z-axis in the background of air. Here D and M denote metal layers and crystal layers with the thicknesses d_D and d_M, respectively, and N is the number of periods. For the metal layers, the relative permittivity and permeability are given by

$$\varepsilon_\mathrm{D} = 1 - \omega_\mathrm{ep}^2/\omega^2, \quad \mu_\mathrm{D} = 1\,, \tag{1}$$

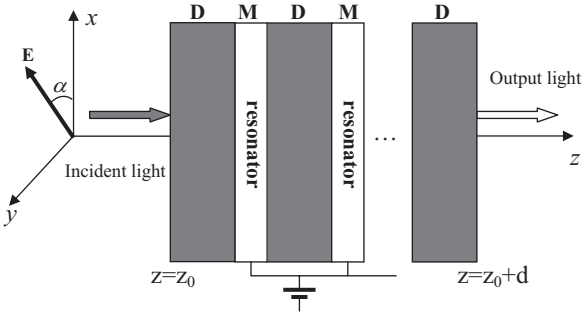

Fig. 1. Schematic of structure. Layers M are composed of magnetic materials and layers D are composed of metal with negative permittivity. An electric field is added on layers M along the direction perpendicular to the z-axis.

where ω_{ep} is the effect electronic plasma frequency. In general, the effective plasma frequency is a function of the electron density and the surface structure, such as subwavelength holes or slits, and is tunable [7]. In design, we keep $\omega_{ep} > \omega$, thus ε_D has a negative value. Due to this negative value, all electromagnetic waves within the layers D are evanescent waves. As is well known, an evanescent wave cannot propagate through a single dielectric layer. For our current structure, if the thicknesses of layers D are very narrow, the evanescent field will be coupled into the first layer M. Because there are evanescent waves in all layers D, the waves within the first layer M undergo total reflection on both its two interfaces. Thus a resonance in a form of standing-wave occurs within the layer M. Similarly, the field energy of the first layer M will be coupled into the second layer M through the evanescent waves within the second layer D, and so on. Therefore, each layer M can be looked at as a resonator cavity, and the whole structure can be looked at as a one dimensional analogy of the coupled-resonators optical waveguides (CROW) through evanescent coupling [8].

2.1. Tight-Binding Analysis

An infinite CROW consisting of an arbitrary type of resonator can be analyzed by the use of the tight-binding approach in analogy to solid-state physics [9–11], in which a propagating mode is expressed as an equiamplitude phase-locked excitation of the local mode of each resonator $\mathbf{E}_\Omega(z)$. In the limit of weak, nearest-neighbour interresonator coupling, the dispersion relation ω_K is

$$\omega_K = \Omega\left[1 - \frac{\Delta\alpha}{2} + \kappa_1 \cos(Kd)\right], \tag{2}$$

where Ω is the resonance frequency of the individual resonator, K is the Bloch wave vector, d is the periodicity, and κ_1 is the coupling factor defined as

$$\kappa_1 = \int [\varepsilon_0(z-d) - \varepsilon(z-d)] \times \mathbf{E}_\Omega(z) \cdot \mathbf{E}_\Omega(z-d)\,\mathrm{d}z. \tag{3}$$

In the current system, the value of κ_1 is determined by the structure parameters of layer D. According to the periodic boundary conditions, K in (2) takes N values (N is the number of cavities M) [12]. Each K corresponds to one eigenfrequency. For N cavities, the single resonant mode Ω is split into N eigenfrequencies and forms a discrete transmission band. Although the tight-binding approach deals with the infinite structure, it can provide an analysis basis on the finite structure.

2.2. Transfer Matrix Analysis

In practice, the number of coupled resonators in a CROW is finite. The transfer matrix method is a powerful tool to study the transmission properties of a layered structure [13, 14]. A monochromatic plane wave with angular frequency ω propagates in the direction of the z-axis with the electric field polarized in an arbitrary direction in the xy-plane having the specific form

$$\mathbf{E} = E_x \mathbf{e_x}\, \mathrm{e}^{\mathrm{i}(k_z z + \omega t)} + E_y \mathbf{e_y}\, \mathrm{e}^{\mathrm{i}(k_z z + \omega t)}, \tag{4}$$

where $\mathbf{e_x}$ and $\mathbf{e_y}$ are unit vectors along the x- and y-axis. The fundamental equations of light are given by Maxwell's equations:

$$\nabla \times \mathbf{E}(\mathbf{r}) = \mathrm{i}\omega\mu_0 \mathbf{H}(\mathbf{r}), \tag{5a}$$

$$\nabla \times \mathbf{H}(\mathbf{r}) = -\mathrm{i}\omega\varepsilon_0 \tilde{\varepsilon} \mathbf{E}(\mathbf{r}). \tag{5b}$$

The specific dielectric tensor $\tilde{\varepsilon}$ in (5b) is given in (6) for anisotropic materials

$$\tilde{\varepsilon} = \begin{bmatrix} \varepsilon_{xx} & 0 & 0 \\ 0 & \varepsilon_{yy} & 0 \\ 0 & 0 & \varepsilon_{zz} \end{bmatrix}. \tag{6}$$

For the metal layers, we set $\tilde{\varepsilon} = \begin{bmatrix} \varepsilon_D & 0 & 0 \\ 0 & \varepsilon_D & 0 \\ 0 & 0 & \varepsilon_D \end{bmatrix}$.

To solve (5), it is convenient to use a state vector defined as $V(z) = [e_x\, e_y\, h_x\, h_y]$. Here, $e_{x(y)}$ and $h_{x(y)}$ are the scaled $x(y)$-components of the electric and magnetic fields, respectively, which are introduced by the relations of $e_{x(y)} = \varepsilon_0 E_{x(y)}$ and $h_{x(y)} = E_{x(y)}/c$ with the vacuum dielectric constant ε_0 and the light vacuum velocity c. Taking (6) into (5), we obtain the following differential equation:

$$\frac{\mathrm{d}}{\mathrm{d}z} V(z) = C \cdot V(z) \tag{7}$$

where $C = \frac{2\pi\mathrm{i}}{\lambda} \begin{bmatrix} 0 & 0 & 0 & 1 \\ 0 & 0 & -1 & 0 \\ 0 & -\varepsilon_{yy} & 0 & 0 \\ \varepsilon_{xx} & 0 & 0 & 0 \end{bmatrix}$. Equation (7) has the eigensolution of $V(z) = V_0 \mathrm{e}^{\lambda z}$. Taking $V(z) =$

$V_0 e^{\lambda z}$ into (7), we obtain

$$(C-\lambda I)V_0 = 0. \tag{8}$$

Equation (8) is a matrix eigenequation and has four eigenvalues and four eigenvectors. Thus (7) has the general solution

$$\begin{aligned} V(z) = {} & A_1\mathbf{a}_1 e^{i\lambda_1 z} + A_2\mathbf{a}_3 e^{i\lambda_2 z} \\ & + A_3\mathbf{a}_3 e^{-i\lambda_3 z} + A_4\mathbf{a}_4 e^{-i\lambda_4 z}. \end{aligned} \tag{9}$$

Here $\mathbf{a}_i$ is the eigenvector corresponding to the eigenvalue λ_i. Therefore (9) can be depicted as

$$V(z) = \overline{a}\cdot e^{i\overline{\lambda}z}\cdot A, \tag{10}$$

where $\overline{a} = [a_1, a_2, a_3, a_4]$ is a 4×4 matrix, $A = [A_1, A_2, A_3, A_4]$, and

$$e^{i\overline{\lambda}z} = \begin{bmatrix} e^{i\lambda_1 z} & & & \\ & e^{i\lambda_2 z} & & \\ & & e^{-i\lambda_3 z} & \\ & & & e^{-i\lambda_4 z} \end{bmatrix}. \tag{11}$$

Equation (10) can be written as

$$\begin{aligned} V(z) &= \overline{a}\cdot e^{i\overline{\lambda}(z-z')}\cdot\overline{a}^{-1}\cdot\overline{a}\cdot e^{i\overline{\lambda}z'}\cdot A \\ &= P_l(z,z')\cdot V(z'), \end{aligned} \tag{12}$$

where $P_l(z,z') = \overline{a}\cdot e^{i\overline{\lambda}(z-z')}\cdot\overline{a}^{-1}$ is called 4×4 transfer matrix, and $l = $ D or M denotes the metal or the crystal layer, z and z' are the positions of two interfaces of the metal or the magnetic layer. The state vector at the incident interface $V(z=z_0)$ and at the exit interface $V(z=z_0+d)$ follow the relation

$$V(z=z_0+d) = P_D P_M P_D P_M P_D V(z=z_0). \tag{13}$$

The angle between the direction of the incident electric field polarization and the x-axis is denoted as α, and the amplitude of the incident electric field is assumed as one. The state vector in the exterior space $z < z_0$ is given by the sum of the incident wave and the two reflected waves as

$$\begin{aligned} V(z) = {} & \begin{bmatrix} \cos\alpha \\ \sin\alpha \\ -\sin\alpha \\ \cos\alpha \end{bmatrix} e^{ik(z-z_0)} \\ & + \left\{ C_1 \begin{bmatrix} \cos\alpha \\ \sin\alpha \\ \sin\alpha \\ -\cos\alpha \end{bmatrix} + C_2 \begin{bmatrix} \sin\alpha \\ -\cos\alpha \\ -\cos\alpha \\ -\sin\alpha \end{bmatrix} \right\} e^{-ik(z-z_0)}, \end{aligned} \tag{14}$$

and in the exterior space $z > z_0 + d$ is given by the sum of the two transmitted waves as

$$\begin{aligned} V(z) = {} & C_3 \begin{bmatrix} \cos\alpha \\ \sin\alpha \\ -\sin\alpha \\ \cos\alpha \end{bmatrix} e^{-ik(z-z_0-d)} \\ & + C_4 \begin{bmatrix} \sin\alpha \\ -\cos\alpha \\ \cos\alpha \\ \sin\alpha \end{bmatrix} e^{-ik(z-z_0-d)}. \end{aligned} \tag{15}$$

The values of $C_1 - C_4$ are related with the amplitudes of the reflected and transmitted waves. We can obtain the values of $C_1 - C_4$ just by taking (14) and (15) into (13). Thus the total state vector at the output point $z = z_0 + d$ can be decomposed in the x- and y-direction and is calculated through

$$\begin{aligned} V(z=z_0+d) &= \begin{bmatrix} E_x \\ E_y \\ H_x \\ H_y \end{bmatrix} (z=z_0+d) \\ &= C_3 \begin{bmatrix} \cos\alpha \\ \sin\alpha \\ -\sin\alpha \\ \cos\alpha \end{bmatrix} + C_4 \begin{bmatrix} \sin\alpha \\ -\cos\alpha \\ \cos\alpha \\ \sin\alpha \end{bmatrix}. \end{aligned} \tag{16}$$

Through (16), we can obtain the transmission properties of the model system.

3. Calculation and Analysis

We choose M as $LiNbO_3$ that is a uniaxial crystal in the absence of an external electric field. Without loss of generality, the refraction indexes of ordinary light and extraordinary light for $LiNbO_3$ are chosen as $n_o = 2.286$ and $n_e = 2.2$, respectively. The optical axis of $LiNbO_3$ is along the direction perpendicular to the z-axis, and the external electric field is along the direction of the optical axis of $LiNbO_3$. According to the crystal optics [15], we can choose the directions of the x- and y-axis to yield

$$n_{xx} = n_o + 1/2 n_o^3 r_{22}\mathbf{E}_\perp = n_o + e, \tag{17}$$

$$n_{yy} = n_o - 1/2 n_o^3 r_{22}\mathbf{E}_\perp = n_o - e, \tag{18}$$

and

$$\varepsilon_{xx} = n_{xx}^2, \tag{19}$$

$$\varepsilon_{yy} = n_{yy}^2, \tag{20}$$

where $e = 1/2n_o^3 r_{22}\mathbf{E}_\perp$ denotes the intensity of the electro-optical effect, and r_{22} is one of the elements of the electro-optical coefficient tensor for $LiNbO_3$. In the numerical studies, we set $\alpha = \pi/4$ and the structure parameters as $\omega_{ep} = 5.4 \cdot 10^{15}\ s^{-1}$, $d_D = 200$ nm, and $d_M = 2500$ nm. Firstly, we let $\mathbf{E}_\perp = 0$ ($e = 0$). In this case, the directions of the x- and y-axis have the same angle of $\pi/4$ with the optical axis. Thus the direction of the electric field of the incident light is perpendicular to the direction of the optical axis, and the incident light becomes o-light. The transmission spectra for the structure $(DM)^N D$ are shown in Figure 2. In the figures, the peaks of E_x and H_y are at the same wavelength just corresponding to one transmission mode called the x-polarization here, while the peaks of E_y and H_x are at the same other wavelength corresponding to the other transmission mode called the y-polarization. For simplicity, we only give the intensities of E_x and E_y. For $N = 1$, there are some discrete single narrow transmission peaks of E_x and E_y with the same intensities of 0.5 at the same wavelengths within wide and deep background of the band gap. For the limit of figure size, only one peak with a Q value of 59 683 is given in the figure (the Q value is the ratio of the center wavelength and the full width at half maximum of the peak). The components of E_x and E_y have no phase difference. Thus the x-polarization and the y-polarization are merged into one polarization with the intensity of 1, and the polarization direction of the output light is the same as that of the incident light. The single resonant mode Ω satisfies the resonant condition

$$n_o d'_M = k\lambda/2, \quad (k = 1, 2, 3, \ldots), \tag{21}$$

where k is the order number of the resonant mode and d'_M is the effective thickness. The resonant peak in Figure 2(a) clearly corresponds to $k = 2$. The two ends of the standing wave are not exactly at the interfaces of layer M but within layer D, i. e., d'_M is a little larger than d_M. For other values of N, there are N resonant peaks of E_x and E_y with the same intensities of 0.5 and no phase difference at the same wavelengths, which means that the single resonant mode Ω is split into N resonant modes due to N cavities. The N resonant modes are just N optical channels. Figure 2(b) shows the result for $N = 7$. All the results can be explained by the tight-binding approach. These discrete resonant peaks with high Q values can be used as multi-channeled filter in DWDM optical communication system.

In future optical communication systems, a multi-channel and compact volume is much needed. Based on the structure of Figure 2(b), we consider the electro-

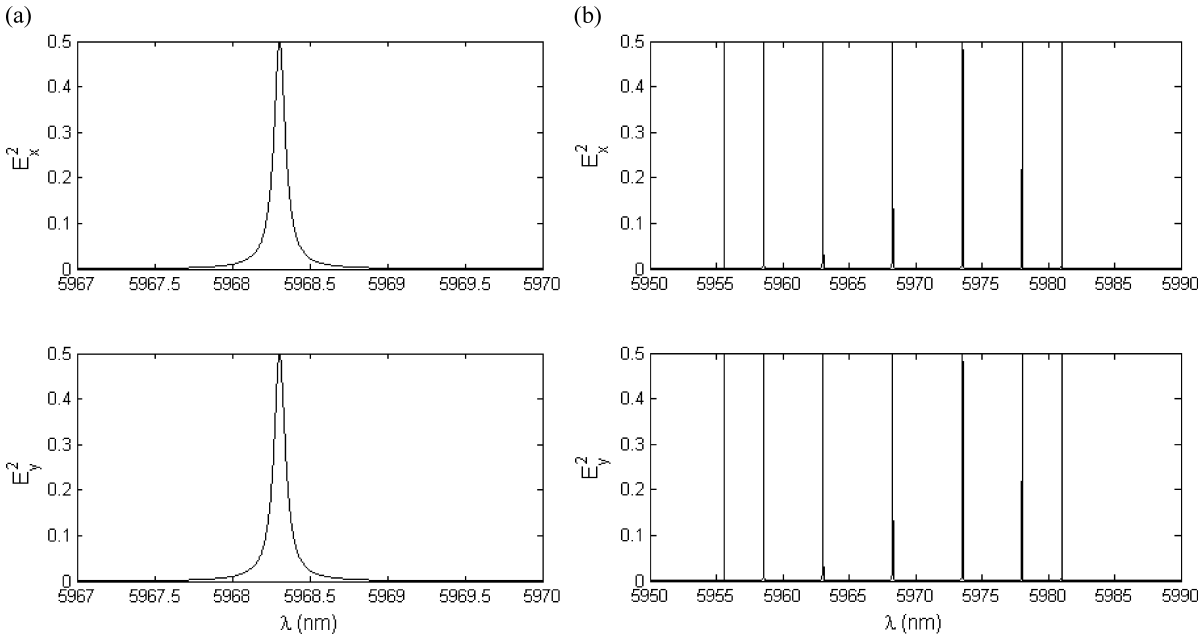

Fig. 2. Transmission spectra for the structure $(DM)^N D$ with $e = 0$. (a) $N = 1$; (b) $N = 7$.

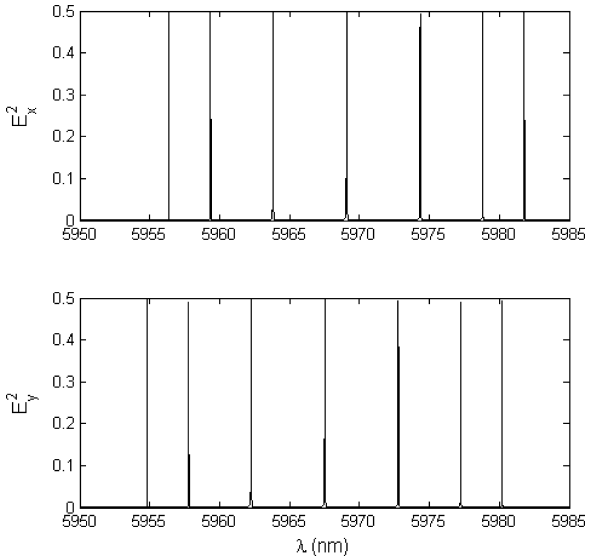

Fig. 3. Transmission spectra of the structure $(DM)^7D$ for $e = 0.0003$.

optic effect, i. e., e is not equal to zero in (17) and (18). Figures 3 and 4 show the transmission spectra of the structure $(DM)^7D$ for $e = 0.0003$ and $e = 0.006$. It is clear that the electro-optic effect makes the x-polarization and the y-polarization split. Thus the total number of channels is two times of that with no electro-optic effect. For the small value of e (Fig. 3), the split interval is small so that the polarization changes alternately from the x-polarization to the y-polarization. However, for the large value of e (Fig. 4), the two groups of x-polarization channels and y-polarization channels are totally separated. Therefore, through the electro-optic effect and the coupled-resonators, we obtain comb-channels with two orthogonal polarizations. Clearly, all these comb-channels have high Q values that cannot be obtained from the defect modes of photonic crystals (PCs). The reason is that the comb-channels come from the effect of resonance and coupling of cavities, while the defect modes of PCs result in the effect of light interference and gap. The Q values of the defect modes of PCs are dependent on the gap depth.

Here we still study the dependence of the split interval of the two orthogonal polarizations on the value of e. From Figure 3, we find that the split intervals for each channel are the same, thus we can only consider the center channel. In Figure 5, we plot the split two orthogonal polarization channels of the center resonant mode with the values of e changing from 0.0003

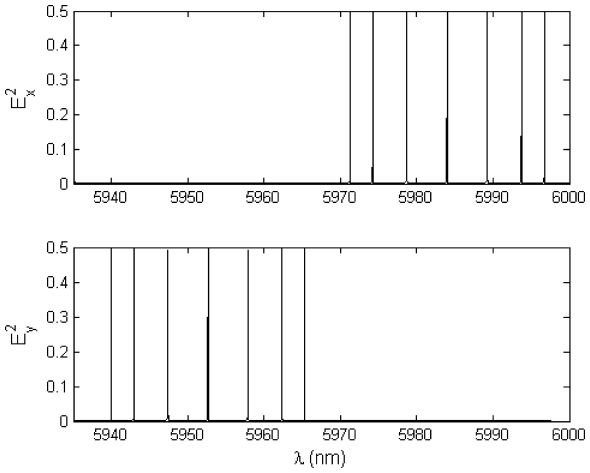

Fig. 4. Transmission spectra of the structure $(DM)^7D$ for $e = 0.006$.

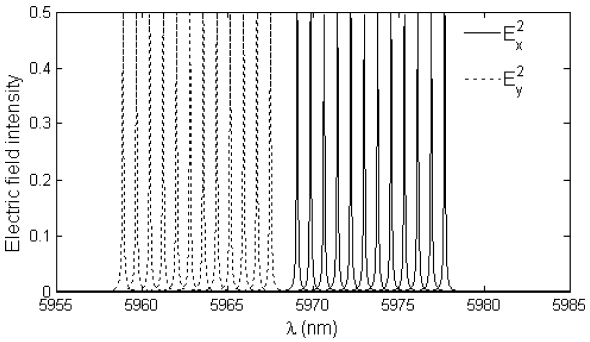

Fig. 5. Split of the center channel with the values of e changing from 0.0003 to 0.0036 by a step size of 0.0003. Each e gives one couple of orthogonal polarization channels. Due to 12 values of e, there are 12 couples of polarization channels.

to 0.0036 by steps of 0.0003. Each e gives one couple of orthogonal polarization channels. Due to 12 values of e, Figure 5 shows 12 couples of polarization channels. The right 12 channels are for the x-polarization, and the left 12 channels are for the y-polarization. The most inner two polarization channels and the most outer two polarization channels correspond to $e = 0.0003$ and $e = 0.0036$, respectively. The split wavelength intervals of the most inner two channels and the most outer two channels are 1.57 nm and 18.79 nm, respectively. Through a detailed observation, we find that the split wavelength interval of two orthogonal polarization channels is linear with the value of e. Thus we obtain

$$\Delta\lambda/\Delta e = 1.5658\,\text{nm}\,, \tag{22}$$

where $\Delta\lambda$ is the split wavelength interval of the two orthogonal polarization channels. Because the value of e is linear with the value of $\mathbf{E}_{\perp}$, we can exactly scale the external electric field through the value of $\Delta\lambda$ and use such structure as an electric field sensor.

4. Conclusions

In this paper, we designed a structure of coupled resonators. Based on the coupling of resonant modes and the electro-optic effect, some orthogonal polarization modes with high Q values are obtained, which can become optical channels. The positions of the x-polarization channels and the y-polarization channels can be adjusted just through adjusting the intensity of the external electric field. Compared with the defect modes of photonic crystals, the structure in this study has a larger number of channels basing on more compact volume. Such structure can be used in DWDM optical communication system and as an electric field sensor.

[1] Y. Li, H. Jiang, L. He, H. Li, Y. Zhang, and H. Chen, Appl. Phys. Lett. **88**, 081106 (2006).
[2] S. Feng, J. Merle Elson, and P. L. Overfelt, Opt. Express **13**, 4113 (2005).
[3] M. Lin, Z. Ouyang, J. Xu, and G. Qiu, Opt. Express **17**, 5861 (2009).
[4] F. Qiao, C. Zhang, J. Wan, and J. Zi, Appl. Phys. Lett. **77**, 3698 (2000).
[5] Y. Xiang, X. Dai, S. Wen, and D. Fan, J. Opt. Soc. Am. A. **24**, A28 (2007).
[6] Y. H. Chen, J. Opt. Soc. Am. B **25**, 1794 (2008).
[7] J. B. Pendry, L. Martín-Moreno, and F. J. Garcia-Vidal, Science **305**, 847 (2004).
[8] A. Yariv, Y. Xu, R. K. Lee, and A. Scherer, Opt. Lett. **24**, 711 (1999).
[9] H. Wang and Y. Fang, Eur. Phys. J. Appl. Phys. **52**, 30703 (2010).
[10] A. Yariv, Y. Xu, R. K. Lee, and A. Scherer, Opt. Lett. **24**, 711 (1999).
[11] N. Stefanou and A. Modinos, Phys. Rev. B **57**, 12127 (1998).
[12] M. Born and K. Huang, Dynamical Theory of Crystal Lattices, Oxford University Press, Oxford 1954.
[13] M. Inoue, K. Arai, T. Fujii, and M. Abe, J. Appl. Phys. **83**, 6768 (1998).
[14] M. Inoue and T. Fujii, J. Appl. Phys. **81**, 5659 (1997).
[15] A. Yariv and P. Yeh, Optical Waves in Crystals: Propagation and Control of Laser Radiation[M], John Wiley & Sons, New York 1984.